ELECTRONIC STRUCTURES AND MAGNETIC PROPERTIES OF RARE-EARTH (Sm,Gd) DOPED Bi$_2$Se$_3$

F. ZHENG[a,b], Q. ZHANG[b*], Q. MENG[b], B. WANG[c,b], L. FAN[b], L. ZHU[b], F. SONG[a], G. WANG[a]
[a]*National Laboratory of Solid State Microstructures, Collaborative Innovation Center of Advanced Microstructures, and Department of Physics, Nanjing University, Nanjing 210093, P. R. China*
[b]*Key Laboratory for Advanced Technology in Environmental Protection of Jiangsu Province, Yancheng Institute of Technology, Yancheng 224051, P. R. China*
[c]*School of Physical Science and Technology, Nanjing Normal University, Nanjing 210023, P. R. China*

First-principles calculations based on density functional theory are performed to investigate the formation energies, band structures, and magnetic properties of rare-earth (RE) metal (Sm, Gd) doped topological insulator Bi$_2$Se$_3$. Our results show that Bi substitutional sites are energetically more favorable for single Gd or Sm impurities. The Sm-doped Bi$_2$Se$_3$ shows a metallic behavior with Sm-f energy band around the Fermi level, while Gd-doped Bi$_2$Se$_3$ exhibits insulating property with a band gap of 0.03eV. As the electron configuration of Gd^{3+} is $4f^7$, its total orbital angular momentum is zero and only spin moment is left, while for Sm^{3+} the net magnetic moment is 3.65μ_B with the low-lying J=7/2 excited state. Further investigation on the magnetic coupling between dopants has suggested that Gd-doped Bi$_2$Se$_3$ tends to be paramagnetic state while Sm-doped Bi$_2$Se$_3$ has a possibility to be ferromagnetic metal, in which easy axis of magnetization lies perpendicular to c-axis.

1. Introduction

In recent years, three-dimensional magnetically-doped topological insulators (MTIs)，which have insulating bulk state and gapless conducting surface states, have always been an interesting subject in experimental and theoretical works.[1-4] The strong spin-orbit coupling (SOC) leads to the nontrivial band topology in these materials, due to these unique properties. MTIs materials have demonstrated their potential application in fast electronic devices, topological quantum computation, and semiconductor spintronics.[5-10] The development of ferromagnetism in MTIs materials is the key to realize the application of semiconductor spintronic devices. Just like other diluted magnetic semiconductors (DMSs)[11-14], the most common way to introduce ferromagnetic order in TIs is through doping with *3d* transition-metal (TM) elements.

The present research mainly focuses on the tetradymite compounds such as Bi$_2$Se$_3$, Bi$_2$Te$_3$ and Sb$_2$Te$_3$. From experimental results, Dyck *et al*.[15] have reported that when Sb$_2$Te$_3$ doped with very low concentration of V (1 to 3%), then the ferromagnetism has been observed with a Curie temperature (T_C) of at least 22 K. Choi *et al*.[16] have also found that Mn-doped Bi$_2$Te$_3$ and Sb$_2$Te$_3$ have ferromagnetic ordering, however, Mn-doped Bi$_2$Se$_3$ showed spin glass behavior. Jung

---

*Corresponding author: qfangzhang@gmail.com

et al. [17] have observed that Fe-doped Bi_2Se_3 exhibited dominance of ferromagnetic interactions, whereas Cr-doped Bi_2Se_3 favored antiferromagnetic interactions, but a ferromagnetism coupling was established in $Cr_x(Bi_2Se_3)_{1-x}$ (x = 0-0.1) films[18] which was found to be mediated by the topological surface states (TSSs), and its onset could be achieved at 20 K. Ferromagnetism was also achieved in $(Bi,Cr)_2(Sb,Te)_3$ films, where robust ferromagnetism was found even though there were no residual carriers.[19] Very recently, Chang *et al.* have further discovered the robust quantum anomalous Hall state in V-doped $(Bi,Sb)_2Te_3$ films,[20] which makes MTIs promising candidates for dissipationless electronic applications. In theoretical part, Larson *et al.* [21] have discovered that when TM (Ti-Zn) atoms doped in Bi_2Se_3, Bi_2Te_3 and Sb_2Te_3, the valence is 3+ for the first half of the series (Ti-Mn) and reduce closer to 2+ (Co) or 1+ (Ni) for the latter half of series. The occurrence of integer moments is also closely related to half-metallic behavior. Zhang *et al.* [22] have reported that 3d TM Cr and Fe-doped Bi_2Se_3 are insulating but the band gaps are substantially reduced due to the strong hybridization between the *d* states of the dopants and the *p* states of the neighboring Se atoms. The Cr doped materials is likely to be ferromagnetic, which agrees with the experimental results[18], while Fe-doped Bi_2Se_3 tends to be weakly antiferromagnetic.

However, in MTIs, the dopant atoms might cause enriched disorders often contribute to some impurity bands in the TI's band gap.[23] Such impurity bands could be very difficult to eliminate and easy to appear in TIs because of their large dielectric constant and Bohr radius.[24] Such a quality limit may be due to the fact that the recent MTIs were produced by introducing transitional metal (TM) dopants including Cr, V, Fe, and Mn.[16-19, 25-27] These atoms are expected to substitute the Bi atoms while their atomic sizes are much smaller than Bi, which leads to versatile defects. In some extreme cases, the TM doping is able to suppress the strength of the spin-orbit coupling (SOC) and damages the topological protection of the TI materials. Rare earth atoms have often large atomic magnetic moments and their atomic size is comparable to Bi. Their SOC is intrinsically strong. Therefore, magnetic doping by rare earth (RE) atoms sheds light on a high-mobility MTI, which may accommodate more exotic topological physics. On the other hand, it is well known that the magnetism of TMs comes from *3d* electrons with a maximum of 5 unpaired electrons. The *3d* electrons are relatively itinerant, in other words, the magnetic dopants may easily lose electrons to the surrounding TI atoms,
which lead to a reduced average moment. A possible way to avoid this problem and enhance the magnetism is to dope TIs with RE metals whose magnetism comes from the *4f* electrons which is more localized than *3d* electrons with a maximum of 7 unpaired electrons. For these reasons, many RE atoms doped (or adsorbed) in Bi_2Se_3 have been performed. Some pioneering attempts on Gd-doped Bi_2Se_3 have found that each Gd^{3+} ion has a magnetic moment as large as ~$6.9\mu_B$ and no hysteresis is observed indicating the sample is paramagnetic (PM)[28]. Bianchi *et al.* [29] have discovered that the intercalation of Rb atoms has almost no effect on the near-surface electronic structure as measure by angle-resolved photoemission spectroscopy. In experiments, we have successfully prepared a new type of DMS-based MTI $(Sm_xBi_{1-x})_2Se_3$. It showed an anisotropic ferromagnetic phase, which exhibited a Curie temperature up to about 52 K and a typical coercive field up to 500 Oe.[30] However, the theoretical research works on RE atoms doped in Bi_2Se_3 are still lacking. Therefore, there is a strong motivation to study the effects of Gd (or Sm) dopants on structural and electronic properties of Bi_2Se_3.

2. Computational methods

All the calculations have been performed using the spin-polarized density functional theory (DFT) with a full-potential linearized augmented plane wave method (FLAPW) embedded in *WIEN2K* code.[31] A generalized gradient approximation (GGA)[32] is used to treat the electron exchange and correlation. Relativistic effects are taken into account in the scalar approximation, and the spin–orbit coupling (SOC) is also taken into account in this present paper. The muffin-tin radii are chosen as 2.6 a.u. for Bi, Se and Sm atoms. The parameter $R_{min}K_{max}$, which controls the size of the basis set in our calculations, is chosen as 6.0. The Brillouin zone (BZ) is represented by

a set of $6\times6\times2$ k-points[33] for the geometry optimizations and for the static total energy calculations. All atoms in the supercell are allowed to relax freely until the maximum Hellmann-Feynman force is smaller than 0.01 eV/Å.

3. Results and discussion

The crystalline Bi_2Se_3 has a rhombohedral structure and its unit cell is composed of three weakly coupled quintuple layers. As shown in Fig. 1, a $2\times2\times1$ supercell containing 24 Bi and 36 Se atoms ($Bi_{24}Se_{36}$) is used to investigate the behaviors of RE atoms dopants in bulk Bi_2Se_3. The lattice parameters were chosen from experimental values of a=4.138 Å and c=28.64 Å[34]. Before and after doped with RE atoms, all atoms are fully relaxed with internal coordinates until residual forces on each atom are less than 0.01 eV/Å.
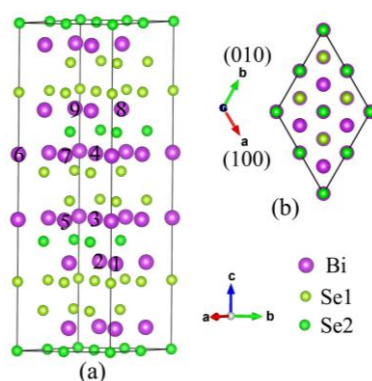

Fig. 1. Structure of a $2\times2\times1$ supercell for modeling dopants in bulk Bi_2Se_3,

the numbers define various configurations of Sm (or Gd)-doped

It is found out that the Se vacancy and substitution are easily introduced in Se1 site from our calculation. This is due to the Se1 layers have larger distance between two quintuple layers, and weakly coupled. Therefore, only Se1 site is considered in our calculations. For comparison, we firstly calculated the formation energies for native defect (V_{Bi} and V_{Se}), RE atoms that is substituted with Sm_{Se} and Sm_{Bi} (or Gd_{Se} and Gd_{Bi}), and RE atoms impurity coupled with native defect $Sm_{Se}+ V_{Bi}$ and $Sm_{Bi}+ V_{Se}$ (or $Gd_{Se}+ V_{Bi}$ and $Gd_{Bi}+ V_{Se}$) which is defined by:

$$\Delta H_f = E_{tot}(RE) - E_{tot}(Bi_{24}Se_{36}) + n_{Bi}\mu(Bi) + n_{se}\mu(Se) - n_{RE}\mu(RE)$$

where, $E_{tot}(RE)$ is the total energy of the supercell with impurity or defect, $E_{tot}(Bi_{24}Se_{36})$ is total energy of the supercell $Bi_{24}Se_{36}$ without any impurity or defect. n_{Bi}, n_{se} and n_{RE} are the corresponding number that have been added or removed from the supercell. The values of $\mu(Bi)$, $\mu(Se)$ and $\mu(RE)$ denote the chemical potentials of Bi, Se and RE (Sm or Gd) atoms, respectively.

The formation energies for these systems vary as a function of chemical potential of Se, which stands for the Se's environment during experimental synthesis. The low and high values of $\mu(Se)$ correspond to the Se-poor and Se-rich growth conditions, respectively. For pure Bi_2Se_3, the $\mu(Bi)$ and $\mu(Se)$ satisfy the following relationships: $2\mu(Bi) + 3\mu(Se) = \mu(Bi_2Se_3)_{bulk}$, $\mu(Se) \leq \mu(Se)_{bulk}$ and $\mu(Bi) \leq \mu(Bi)_{bulk}$, where $\mu(Se)_{bulk}$, $\mu(Bi)_{bulk}$ and $\mu(Bi_2Se_3)_{bulk}$ refer to the chemical potentials of stable Bi, Se and Bi_2Se_3 crystals. In our calculations, the $\mu(Se)$ in the Se-rich growth condition is defined as $\mu(Se)_{bulk}$, while the $\mu(Bi)$ is determined by $(\mu(Bi_2Se_3)_{bulk} - 3\mu(Se)_{bulk})/2$. In the Se-poor growth condition, the $\mu(Bi)$ amount to the energy of Bi crystal ($\mu(Bi)_{bulk}$) and $\mu(Se)$ is calculated from $(\mu(Bi_2Se_3)_{bulk}-2\mu(Bi)_{bulk})/3$.

Through analyzing the formation energies of the native defects (V_{Bi} and V_{Se}) in Fig. 2.a, It can be seen that in Se-poor growth conditions, native defect V_{Se} is energetically favorable than the V_{Bi}. The native defect V_{Se} formation energies increased from 1.14 to 2.16 eV when the growth conditions from Se-poor to Se-rich. To the contrary, the V_{Bi} formation energies decreased from 4.13 to 2.60 eV. In Sm-doped system, the formation energies of $Sm_{Se} + V_{Bi}$ and Sm_{Bi} decreased when the growth conditions from Se-poor to Se-rich, while $Sm_{Bi} + V_{Se}$ and Sm_{se} formation energies increased. The formation energies of V_{Bi} and Sm_{se} are positive and higher than other defects, indicating that V_{Bi} and Sm_{se} are hence quite unstable. On the other hand, the formation energies of Sm_{Bi} are negative, resulting in spontaneous formations in experiments. In Fig. 2.b, the formation energies change of the Gd-doped systems trend almost the same as Sm-doped systems. The formation energies are negative for Sm_{Bi} and Gd_{Bi} systems, their formation energies are always lower than other systems and the lowest formation energies are -4.578 and -5.24 for Sm_{Bi} and Gd_{Bi} at Se-rich condition, respectively. This implies that Sm_{Bi} and Gd_{Bi} system are energetically favorable and can be easily achieved in experiments under the Se-rich condition. From experiments, Song *et al*.[28] have found that Gd dopants mainly prone to substitute Bi atoms. More importantly, we have prepared $(Sm_xBi_{1-x})_2Se_3$ crystals with different doping concentrations of $x = 0$, 0.002, 0.005, 0.025, and 0.05 in experiments.[30]
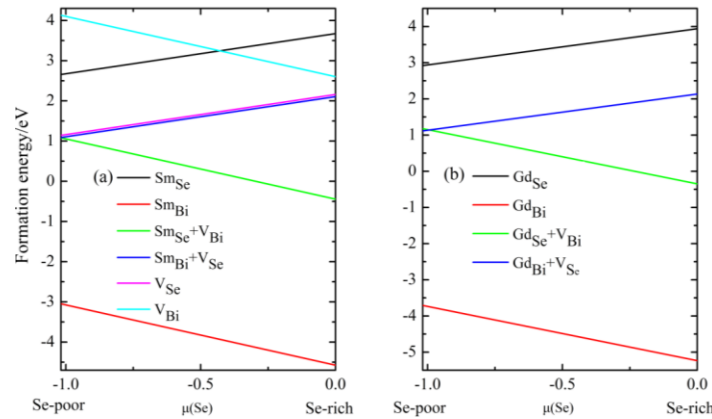

Fig. 2. The calculated relative formation energy for Bi_2Se_3 as a function of the Se-poor and Se-rich chemical potentials. (a) Sm systems and (b) Gd systems.

We firstly consider a single Bi atom on the 3th site substituted by Sm (or Gd) atom as shown in Fig. 1a, which would lead to Sm (or Gd) doping concentration of 4.17%. All atomic positions are fully relaxed after replacing one Bi atom with Sm (or Gd) atom. As shown in Fig. 3, the pristine $Bi_{24}Se_{36}$ calculated without SOC has a direct band gap which is about 0.19 eV, and it turns to indirect band gap which is about 0.27 eV with SOC. Our results are consistent with the previous calculations[22, 35] and experimental data (about 0.2-0.3 eV[36,37]). Comparing the band structure without and with SOC, It can be seen that only qualitative change has an anti-crossing feature around Gamma point, which is induced by turning on SOC. An inversion between the conduction band and valence band is an indication that it is a topological insulator. The calculated bond lengths of Bi-Bi are all 4.138Å, which are smaller than the Bi-Sm bond lengths of 4.146 Å and Bi-Gd bond lengths of 4.147 Å. The Bi-Sm (or Gd) bond lengths are larger than that of Bi-Bi due to the ionic radius of Sm^{3+} (or Gd^{3+}), which is larger than that of Bi^{3+}.
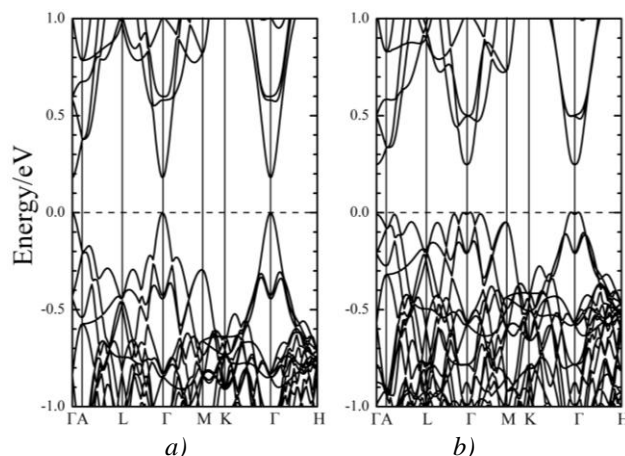
Fig. 3. Band structure of Bi₂Se₃ calculated for a 2×2×1 supercell (a) without and (b) with SOC.

As it can be seen from Fig. 4.a, the calculated band structure of $Bi_{23}SmSe_{36}$ with SOC exhibits a metallic behavior with bands crossing the Fermi level (E_f), while for $Bi_{23}GdSe_{36}$, it is also an insulator with a gap about 0.03 eV in Fig. 6.a. In $Bi_{23}SmSe_{36}$ system, the spin, orbital and net magnetic moments of cations Sm^{3+} are 5.21, -1.56 and $3.65\mu_B$, respectively. In theory, the ground electronic state of Sm^{3+} can be described by Hund's Rule as $^6H_{5/2}$. Since the 4f electron number is less than half filled, the total angular momentum has J=| L-S| , so there is only a small net magnetic moment of $0.84\mu_B$. There is a big discrepancy between our results and the theoretical value. Dhesi *et al*. [38] have demonstrated the exchange and crystal-field interactions mix the low-lying *J*=7/2 excited state into the Sm f^5 $^6H_{5/2}$ ground state. And Mazzone *et al*. [39] also pointed that for the excited *J*=7/2 level, the calculated magnetic moment is $3.28\mu_B$, which is consistent with our result net magnetic moment of $3.65\mu_B$. More importantly, our further calculations demonstrated the anisotropic magnetism of Sm-doped Bi_2Se_3 system. The magnetic anisotropy energy out-of-plane (001) is larger than that in-plane (100), (010), (110) direction about 10 meV, which confirms the in-plane easy axis. In experiments, our measurements also demonstrated the anisotropic magnetism of the samples, where the in-plane coercive field was larger than the out-of-plane coercive field. [30] The observations confirm the in-plane easy axis which agrees with our calculations. In $Bi_{23}GdSe_{36}$ system, the spin magnetic moment of the cations Gd^{3+} is about $6.744\mu_B$ and the orbital magnetic moment is about $0.07\mu_B$. Since the electron configuration of Gd^{3+} is $4f^7$, that is to say half-filled (ground state is $^8S_{7/2}$ form Hund's Rule), its total orbital angular momentum is zero and only spin magnetic moment is left (for which the spin moment dominates or the orbital moment is absent).
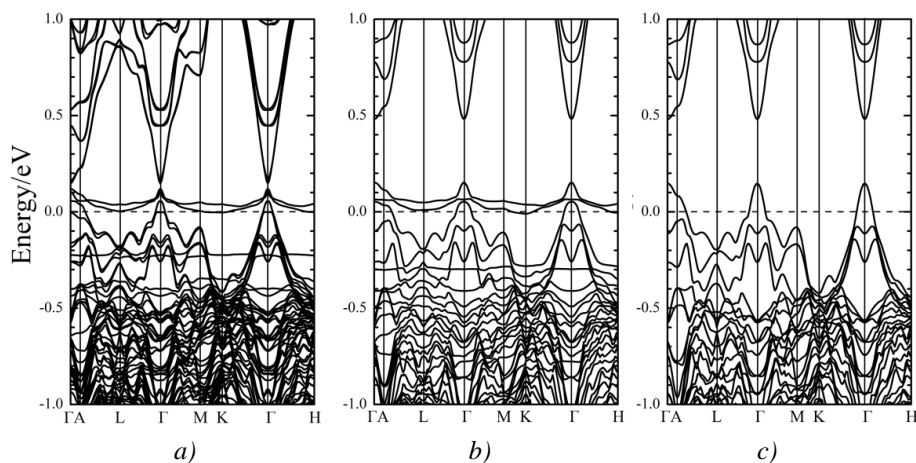

Fig. 4. Band structure of Bi₂Se₃ calculated for a 2×2×1 supercell doped with

a Sm atom (Bi₂₃SmSe₃₆) (a) with SOC (b) spin-up (c) spin-down

In Fig. 4b-c present the band structures of $Bi_{23}SmSe_{36}$ with spin-polarized. The spin-up and spin-down channels have shown metallic properties, since the bands cross the Fermi level (E_f). In spin-up channels, there are two flat impurity bands above E_f which are unoccupied, and five flat impurity bands below E_f which are occupied. The materials have displayed a magnetic metallic behavior with total magnetic moment of $5.1\mu_B$ due to different between spin-up and spin-down channel. In $Bi_{23}SmSe_{36}$ system, the magnetic moments of the Sm is about $5.34\mu_B$, and other atoms have a smaller magnetic moments (about $0.001~0.04\mu_B$) align antiparallel with the moments of Sm atom. A metal–insulator transition occurs when the Sm atom is incorporated into the pristine system. The spin-polarized which are calculated for total and partial density of states (DOS) in $Bi_{23}SmSe_{36}$, Bi atom, and Sm-f state are shown in Fig. 5. The $Bi_{23}SmSe_{36}$ system is magnetic because the spin-up and spin-down branches are being unequal around E_f with magnetic moment of $5.1\mu_B$. The E_f goes into valance band in the spin-up and spin-down channel, indicating that the system belongs to magnetic metallic. From the DOS of Bi atom, we can see that the spin-up and spin-down branches are almost being equal, so Bi atom has little effect for the system. It is highlighted that for the DOS of Sm-f, there is a large splitting of the energy level near the E_f due to the quantum mechanical level repulsion. The spin-up states are partial filled, and the spin-down states are fully unoccupied, resulting in a total magnetic moment of $5.34\mu_B$ of Sm, which almost contributed by the Sm-f orbitals. In consistent with band structures analysis above, it is most important to note that the flat impurity bands around the E_f, which are all from the Sm-f orbitals.
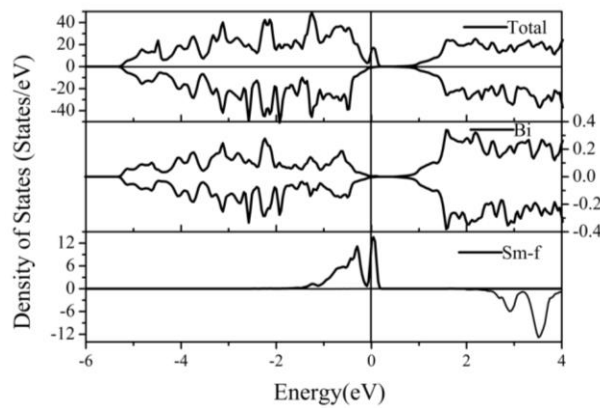

Fig. 5. DOS of $Bi_{23}SmSe_{36}$ with single Sm substitution for Bi: (a) Total DOS;

Partial DOS for (b) Bi and (c) Sm-f

In Fig. 6b-c present the band structures of $Bi_{23}GdSe_{36}$ with spin-polarized. We can see that the spin-up and spin-down channels all have a band gap about 0.35eV. Different from the $Bi_{23}SmSe_{36}$ shows metallic properties, the $Bi_{23}GdSe_{36}$ has still been an insulator. From band structures, it is important to note that there are flat impurity bands at 4.24 eV below E_f all occupied and similar bands at 0.9 eV above E_f are all unoccupied. Comparing with the DOS, the flat impurity bands occupied or unoccupied are all come from the Gd-f states. The spin-up states are fully occupied but the spin-down states are partial filled, resulting in a total magnetic moment of $7.02\mu_B$. The magnetic moments almost come from the Gd atom, and the magnetic moment of the Gd is about $6.91\mu_B$[28], which is equal to the Gd-f occupied electrons numbers. It means that the Gd^{3+} has a spin S=7/2, and the 4f electrons are responsible for the magnetism in rare earth metals. $Bi_{23}GdSe_{36}$ can be used for diluted magnetic semiconductors in spintronics because it is large magnetic moment.
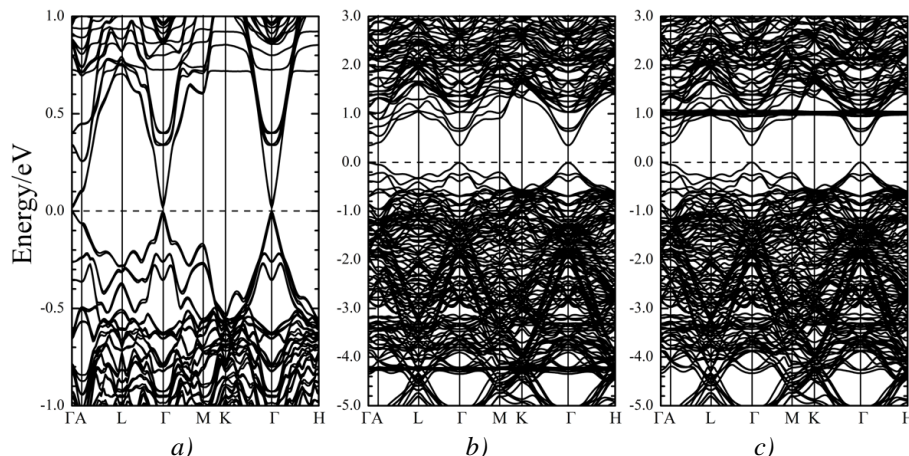
Fig. 6 Band structure of Bi_2Se_3 calculated for a $2\times2\times1$ supercell doped with
a Gd atom ($Bi_{23}GdSe_{36}$) (a) with SOC (b) spin-up (c) spin-down
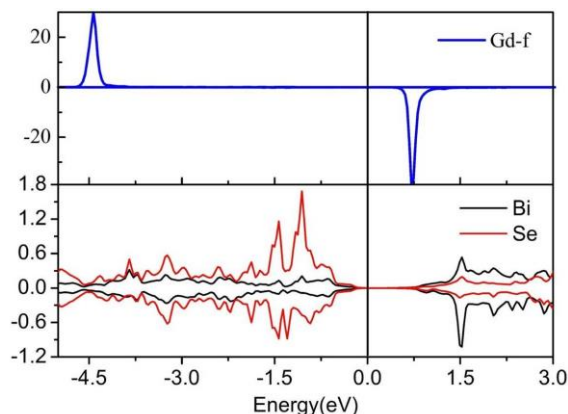

Fig. 7 Partial DOS of $Bi_{23}GdSe_{36}$ with single Gd substitution for Bi: (a) Gd-f,
(b) Bi and Se atom

To study the magnetic interaction in system, seven different configurations of two Sm (or Gd)-doped $Bi_{24}Se_{36}$ have been calculated, in which two Bi atoms are substituted by two Sm (or Gd) atoms. We use (i, j) to denote a Sm-Sm (or Gd-Gd) pairs, in which two Bi sites are removed at i and j sites as shown in Fig.1 and Table1 (Table 2). The magnetic coupling strength can be obtained from the energy difference between ferromagnetic (FM) and antiferromagnetic (AFM) states ($\varDelta E = E_{AFM} - E_{FM}$). $\Delta\varepsilon$ is the relative energy with respect to the ground state of configuration III(2,5) for Sm-doped system and II(2,3) for Gd-doped system. For Sm-doped system in Table 1, it is found that the configuration I, II, III and IV are most stable case with FM state. In configuration III, the two Sm atoms are separated by other atoms with a distance of 5.915 Å with relatively lower energy than other configurations, thus the FM order is the stable ground state. In experiment, we find an intrinsic Sm-dopant-induced ferromagnetism in the sample with a Curie temperature of 52 K and a coercive field of as high as 500 Oe,[30] which agrees well with our computed result. The ferromagnetism order with high Curie temperature is achieved upon doping Sm atoms, which may act as an ideal platform for robust topological edge transport and spintronic device applications.[30] In Gd-doped system, the PM state is stable in all case, which agrees with experimental observations of PM state[28], and the configurations II(2,3) is ground state with the Gd atoms distance of 4.301 Å. The Ruderman-Kittle-Kasuya-Yosida (RKKY) interaction is responsible for the magnetic ordering of the systems [28,30].

Table 1 The calculated result for all the configurations of $Bi_{22}Sm_2Se_{36}$. The relative energy $\Delta\varepsilon$ is the total energy of the $Bi_{22}Sm_2Se_{36}$ with respect to the ground state of configurations III(2,5). ΔE is the FM stabilization energy between the AFM and FM states for each configuration. The optimized Sm-Sm distance is d_{Sm}.

$Bi_{22}Sm_2Se_{36}$	d_{Sm}(Å)	ΔE(meV)	$\Delta\varepsilon$(meV)	Magnetic coupling
I(1,2)	4.138	39.83	72.06	FM
II(2,3)	4.279	21.85	16.40	FM
III(2,5)	5.915	12.37	0.00	FM
IV(3,4)	6.027	13.81	36.62	FM
V(2,6)	9.842	1.71	35.92	PM
VI(2,7)	10.673	0.15	41.71	PM
VII(2,8)	13.332	-2.14	44.56	PM
VII(2,9)	13.955	1.88	33.28	PM

Table 2. The calculated result for all the configurations of $Bi_{22}Gd_2Se_{36}$. The relative energy $\Delta\varepsilon$ is the total energy of the $Bi_{22}Gd_2Se_{36}$ with respect to the ground state of configurations II(2,3). ΔE is the FM stabilization energy between the AFM and FM states for each configuration. The optimized Gd-Gd distance is d_{Gd}.

$Bi_{22}Gd_2Se_{36}$	d_{Gd}(Å)	ΔE(meV)	$\Delta\varepsilon$(meV)	Magnetic coupling
I(1,2)	4.138	-1.13	21.82	PM
II(2,3)	4.301	1.30	0.00	PM
III(2,5)	5.886	1.25	26.82	PM
IV(3,4)	5.998	1.67	11.22	PM
V(2,6)	9.836	-1.05	14.15	PM
VI(2,7)	10.642	0.15	24.27	PM
VII(2,8)	13.326	-0.61	27.45	PM
VII(2,9)	13.982	0.52	33.28	PM

4. Conclusions

In summary, the electronic structures and magnetic properties of rare earth metal Sm and Gd-doped in topological insulator Bi_2Se_3 have been studied by first-principle calculation. Our calculated formation energies have indicated that Bi substitutional sites were strongly preferred by Sm or Gd atoms at Se-rich condition. From SOC calculation, it was found that $Bi_{23}SmSe_{36}$ showed metallic properties, while $Bi_{23}GdSe_{36}$ was still a topological insulator with energy gap of 0.03 eV. For Sm^{3+} the net magnetic moment was $3.65\mu_B$ with the low-lying J=7/2 excited state, and the magnetic moment of the cations Gd^{3+} was about $6.744\mu_B$, because the Gd^{3+} orbital moment is absent and only spin magnetic moment is left. This indicates a potential application for fabricating strong magnetic TI in spintronics. The calculated magnetic coupling between dopants have suggested that Sm doped Bi_2Se_3 is likely FM state, while the Gd doped system showed PM state. Thus, the anisotropic magnetism of Sm-doped Bi_2Se_3 system have been demonstrated and the easy axis of magnetization was lied in-plane which agreed with the experimental result.

Acknowledgments

References

[1] L. Fu, C. L. Kane, and E. J. Mele, Phys. Rev. Lett. **98**, 106803 (2007).
[2] R. Roy, Phys. Rev. B **79,** 195332 (2009).
[3] J. E. Moore and L. Balents, Phys. Rev. B **75**, 121306 (2007).
[4] H. Zhang, C.-X. Liu, X.-L. Qi, X. Dai, Z. Fang, S.-C.Zhang, Nat. Phys. **5**, 438 (2009).
[5] L. Fu and C. L. Kane, Phys. Rev. Lett. **100**, 096407 (2008).
[6] A. R. Akhmerov, J. Nilsson, C. W. J. Beenakker, Phys. Rev. Lett. **102**, 216404 (2009).
[7] J. D. Sau, R. M. Lutchyn, S. Tewari, and S. Das Sarma, Phys. Rev. Lett.**104**, 040502 (2010).
[8] M. Z. Hasan and C. L. Kane, Rev. Mod. Phys. **82**, 3045 (2010).
[9] D. Hsieh, D. Qian, L. Wray, Y. Xia, Y. S. Hor, R. J. Cava, and M. Z.Hasan, Nature (London) **452**, 970 (2008).
[10] D. Hsieh, Y. Xia, L. Wray, D. Qian, A. Pal, J. H. Dil, J. Osterwalder, F. Meier, G. Bihlmayer, C. L. Kane et al. Science 323, 919 (2009).
[11] H. Ohno, Science **281,** 951 (1998).
[12] J. K. Furdyna, J. Appl. Phys. **64**, R29 (1988).
[13] T. Fukumura, Z. Jin, A. Ohtomo, H. Koinuma, and M. Kawasaki, Appl. Phys. Lett. **75,** 3366 (1999).
[14] K. Sato, H. K. Yoshida, Jpn. J. Appl. Phys. Part 2 **39,** L555 (2000).
[15] J. S. Dyck, P. H´ajek, P. Loˇst'´ak, and C. Uher, Phys. Rev. B 65,115212 (2002).
[16] J. Choi, H.-W. Lee, B.-S. Kim, S. Choi, J. Choi, J. H. Song, and S. Cho, J. Appl. Phys. **97**, 10D324 (2005).
[17] Y. H. Choi, N. H. Jo, K. J. Lee, J. B. Yoon, C. Y. You and M. H. Jung J. Appl. Phys. **109**, 07E312 (2011).
[18] J. G. Checkelsky, J. T. Ye, Y. Onose, Y. Iwasa, Y. Tokura, Nature Phys. 8, 729(2012).
[19] C. Z. Chang, J. S. Zhang, X. Feng, J. Shen, Z. C. Zhang, M. H. Guo, K. Li, Y. B. Ou, P. Wei, L. L. Wang, Z. Q. Ji, Y. Feng, S. H. Ji, X. Chen, J. F. Jia, X. Dai, Z. Fang, S. C. Zhang, K. He, Y. Y. Wang, L. Lu, X. C. Ma, Q. K. Xue, Science 2013, 340, 167.
[20] C. Z. Chang, W. W. Zhao, D. Y. Kim, H. J. Zhang, B. A. Assaf, D. Heiman, S. C. Zhang, C. X. Liu, M. H. W. Chan, J. S. Moodera, Nature Mater. 14, doi:10.1038/nmat4204 (2015).
[21] P. Larson and Walter R. L. Lambrecht, Phys. Rev. B 78, 195207(2008).
[22] J. M. Zhang, W. Zhu, Y. Zhang, D. Xiao, Y. Yao, Phys. Rev. Lett. **109**, 226405 (2012).
[23] Z. Ren, A. A. Taskin, S. Sasaki, K. Segawa, Y. Ando, Phys. Rev. B82, 241306 (**2010**).
[24] G. Zhang, H. J. Qin, J. Chen, X. Y. He, L. Lu, Y. Q. Li, K. H. Wu, Adv. Funct. Mater **21**, 2351(2011).
[25] J. J. Cha, M. Claassen, D. S. Kong, S. S. Hong, K. J. Koski, X. L. Qi, Y. Cui, Nano Lett. **12**, 4355 (2012).
[26] H. J. Kim, K. S. Kim, J. F. Wang, V. A. Kulbachinskii, K. Ogawa, M. Sasaki, A. Ohnishi, M. Kitaura, Y. Y. Wu, L. Li, I. Yamamoto, J. Azuma, M. Kamada, V. Dobrosavljevic, Phys. Rev. Lett. **110**, 136601(2013).
[27] C. Z. Chang, P. Z. Tang, Y. L. Wang, X. Feng, K. Li, Z. C. Zhang, Y. Y. Wang, L. L.Wang, X. Chen, C. X. Liu, W. H. Duan, K. He, X. C. Ma, Q. K. Xue, Phys. Rev. Lett. **112**, 056801(2014).
[28] Y. R. Song, F. Yang, M. Y. Yao, F. F. Zhu, L. Miao, J. P. Xu, M. X. Wang, H. Li, X. Yao, F. H. Ji, S. Qiao, Z. Sun, G. B. Zhang, B. Gao, C. H. Liu, D. Qian, C. L. Gao, J. F. Ji*a,*

Appl. Phys. Lett. **100**, 242403(2012).

[29] M. Bianchi, R. C. Hatch, Z. Li, P. Hofmann, S. Fei, J. Mi, et al. Acs Nano **6**(8), 7009 (2012).

[30] T. S. Chen, W. Q. Liu, W., Zheng, F. B. Zheng, M. Gao, X. C. Pan, C. Laan, X. F. Wang, Q. F. Zhang, F. Q, Song, B. G. Wang, B. L. Wang, Y. B. Xu, G. H. Wang, R. Yong. Advanced Materials, **27**(33), 4823.

[31] K. Schwarz, P. Blaha, Comput. Mater. Sci. **28**, 259 (2003).

[32] J. P. Perdew, K. Burke, Ernzerhof, M. Phys. Rev. Lett. **77**, 3865 (1996).

[33] L.H. Ye, A.J. Freeman, B. Delley, Phys. Rev. B **73,** 033203 (2006).

[34]R. W. G. Wyckoff, Crystal Structure,Vol.2. John Wiley and sons, New York (1964).

[35] H. Zhang, C. Liu, X. Qi, X. Dai, Z. Fang, S. Zhang. Nature Phys. **5**, 438 (2009).

[36]Black, J., Conwell, E. M., L. Seigle, C. W. Spencer, J. Phys. Chem. Solids **2**, 240 (1957).

[37]Mooser, E. & Pearson, W. B. Phys. Rev. **101**, 492 (1956).

[38] S. S. Dhesi, G. van der Laan, P. Bencok, N. B. Brookes, R. M. Galéra, P. Ohresser. Phys. Rev. B **70,** 134418 (2004).

[39] D. Mazzone, P. Riani, M. Napoletano, F. Canepa, Journal of Alloys and Compounds **387**, 15(2005).